Metallization of hydrogen using heavy-ion-beam implosion of multilayered cylindrical targets

N. A. Tahir, D. H. H. Hoffmann, A. Kozyreva, and A. Tauschwitz

Institut für Kernphysik, Technische Universität Darmstadt, Schlossgarten Strasse 9, D-64289 Darmstadt, Germany

A. Shutov

Institute for Chemical Physics Research, Chernogolovka, Russia

J. A. Maruhn

Institut für Theoretische Physik, Universität Frankfurt, D-60054 Frankfurt, Germany

P. Spiller, U. Neuner, J. Jacoby, M. Roth, and R. Bock

Gesellschaft für Schwerionenforschung, Planckstrasse 1, D-64291 Darmstadt, Germany

H. Juranek and R. Redmer

Fachbereich Physik, Universität Rostock, Universitätsplatz 3, 18051 Rostock, Germany

Employing a two-dimensional simulation model, this paper presents a suitable design for an experiment to study metallization of hydrogen in a heavy-ion beam imploded multilayered cylindrical target that contains a layer of frozen hydrogen. Such an experiment will be carried out at the upgraded heavy-ion synchrotron facility (SIS-18) at the Gesellschaft für Schwerionenforschung, Darmstadt by the end of the year 2001. In these calculations we consider a uranium beam that will be available at the upgraded SIS-18. Our calculations show that it may be possible to achieve theoretically predicted physical conditions necessary to create metallic hydrogen in such experiments. These include a density of about 1 g/cm^3, a pressure of 3–5 Mbar, and a temperature of a few 0.1 eV.

I. INTRODUCTION

Intense beams of energetic heavy ions can generate extended volumes of high-energy-density plasmas with lifetimes of the order of hundreds of ns. These samples of heavy-ion generated plasmas can be used to study the equation-of-state (EOS) properties of matter under such extreme conditions. In previous publications [1–3] we presented optimized design for a number of suitable heavy-ion-matter interaction experiments to create high-energy-density matter in the laboratory. These design studies were carried out using a two-dimensional hydrodynamic simulation model, BIG-2 [4]. These include simulation of hydrodynamic and thermodynamic response of beam heated ''sub-range'' [1] as well as ''super-range'' [2] cylindrical targets. In the former case, the cylinder length is considered to be much less than the range of the driver ions whereas in the latter case the cylinder length is significantly larger than the ion range. We also presented calculations using an ion beam that has an annular focal spot (a ring-shaped focal spot) that interacts with solid as well as hollow cylinders [3].

The above beam-target interaction experiments will be performed at the GSI Darmstadt after the completion of the upgrade of the existing synchrotron facility (SIS-18). This upgrade is expected to be completed by end of the year 2001 and it includes introduction of a high current injector [5] and a powerful rf-buncher [6]. The new high current injector that is based on a radio frequency quadrupole and IH (interdigital H-mode) structure has already become operational providing argon as well as uranium ions. So far, a maximum number of

3×10^{10} ions of 300 MeV/u argon and about 10^9 ions of uranium 200 MeV/u have been accelerated in separate operations. The beam intensity is expected to increase steadily due to further optimization of accelerator parameters and the number of uranium 200 MeV/u particles will increase to 2×10^{11}. The pulse length at present is of the order of 300 ns that will be reduced to 50 ns due to bunch compression performed by the rf-buncher. The upgraded SIS-18 parameters lead to specific power deposition of about 1–2 TW/g in solid matter that according to our simulations [7] will heat solid matter to about 10 eV.

Another very interesting and important experiment that will be performed at the upgraded SIS-18 is to study the possibility of creating metallic hydrogen in appropriately designed multilayered targets imploded by the ion beam. This paper presents design of such an experiment providing target configuration and parameters that have been optimized with respect to the SIS-18 beam. As shown in Fig. 1, the target consists of a cylinder of frozen hydrogen with a radius R_h and a length L. The hydrogen is enclosed in a thick cylindrical shell of solid lead whose outer radius is R_o. The right face of this target is irradiated by a beam that has an annular or ring-shaped focal spot. It has been shown [3] using a particle tracking computer program that it is possible to create such a beam focal spot employing a plasma lens. The proposed beam-target geometry for this experiment has been arranged in such a manner that the inner radius of the beam focal spot, R_{bi} is $\geqslant R_h$ and the outer ring radius, R_{bo} is less than the target outer radius, R_o. This avoids direct irradiation of the frozen hydrogen and only a part of the lead shell
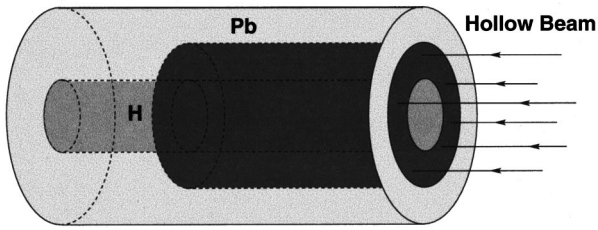
FIG. 1. Design of a multilayered heavy-ion-imploded target for creating metallic hydrogen.

is heated. The heated lead then implodes inwards, slowly compressing the hydrogen. Employing the BIG-2 code we have simulated hydrodynamic and thermodynamic response of the above target using the upgraded SIS-18 beam. Our simulations show that it may be possible to achieve theoretically predicted physical conditions required to metallize hydrogen, namely, a density of about 1 g/cm^3, a pressure of 3–5 Mbar and a temperature of a few 0.1 eV.

In Sec. II we present a general discussion on the problem of hydrogen metallization while the simulations results are given in Sec. III. The conclusions drawn from this work are presented in Sec. IV.

Gesellschaft für Schwerionenforschung (GSI) is also considering as a possible scenario for future development of the accelerator facility to build a synchrotron with a much higher magnetic rigidity of 200 Tm (SIS-200). Preliminary design studies show that the beam delivered by such a facility will consist of at least 10^{12} ions of U^{+10} with a maximum particle energy of 1 GeV/u. Since it is also possible to operate such a machine at lower particle energies, we have carried out a calculation using the SIS-200 beam, but considering a particle energy of 400 Mev/u which is more appropriate for such experiments.

II. A DISCUSSION OF HYDROGEN METALLIZATION

Creation of metallic hydrogen by application of high pressure has been a subject of great importance since its theoretical prediction by Wigner and Huntigton in 1935 [8]. In their original treatment they predicted that the normal molecular hydrogen, which is an insulator, will transform to a monoatomic metallic system when subjected to a pressure of 0.25 Mbar. More recently, an alternative picture has been proposed according to which the insulator molecular solid first transforms to a metallic state, remaining a molecular solid under the influence of the applied pressure. This metallization occurs due to an overlap of the valence and conduction bands [9,10]. As the density is further increased, molecular dissociation takes place that leads to an atomic metallic state.

The critical pressure of 0.25 Mbar predicted by Wigner and Huntigton is certainly incorrect because experiments have exceeded 2 Mbar without detecting such a state successfully. Modern estimates predict that this transition will occur at pressures of 3–5 Mbar and at a density of around 1 g/cm^3 while the temperature should be a few 0.1 eV.

Properties of hydrogen under extreme conditions are of importance to inertial fusion and for interiors of giant planets, such as Saturn and Jupiter. Moreover, it has been pre-

dicted by different researchers that metallized hydrogen may have exotic properties with useful applications. For example, it has been predicted by Ashcroft [11] that metallic hydrogen may be a room temperature superconducting material. Also if it could be stabilized after release of the applied pressure, the metallic hydrogen could be an efficient and clean technological fuel, in particular for rocket propulsion. It has been suggested by Brovman *et al.* [12] that once created, metallic hydrogen may be metastable and the sample would remain intact after the removal of the pressure.

Due to the many exciting predictions for highly compressed hydrogen, extensive experimental effort has been devoted during the past few decades to study this problem. Different techniques including employment of diamond anvil cell [13,14] and gas guns [15,16], samples of hydrogen have been strongly compressed to achieve metallization. Although significant progress has been made in this field, the final goal has still not been achieved.

Intense beams of energetic heavy ions provide us with an additional tool to investigate the interesting problem of hydrogen metallization. High pressures generated due to ion beam energy deposition seem to be sufficient to implode the target to the required high densities. The time scale for heavy-ion driven compression is of the order of hundred ns, which leads to a slow implosion that allows a near isentropic compression. At the same time this time is short enough to avoid any significant diffusion of hydrogen into the confining lead shell. In Sec. III we present detailed two-dimensional hydrodynamic simulation results using suitable multilayered heavy-ion imploded targets that can be used at the GSI accelerator facility.

III. SIMULATION RESULTS

The heavy-ion synchrotron at the GSI Darmstadt is a unique facility worldwide that delivers intense beams of energetic heavy ions. Using the existing facility, interesting experimental work has been carried out during the past decade in the field of heavy-ion matter interaction. This included measurement of energy loss of ions in plasma, studies of charge state of projectile ions in the target, heating of solid crystals with ion beams and studies of ion-beam-induced hydrodynamics [17–23]. However, in these experiments lighter heavy ions like neon and argon were used and the pulse duration was quite long, 300–500 ns. The corresponding specific power deposition was very low that in turn lead to low target temperatures of a few thousand K.

The upgraded synchrotron SIS-18 would deliver a U^{+28} beam having a total number of 2×10^{11} ions with a particle energy of 200 MeV/u. The pulse duration will be 50 ns and the beam power deposition profile along the radial direction will be a Gaussian with a full width at half maximum of 1.0 mm, that can be regarded as the effective beam radius.

GSI is also considering a proposal to build a synchrotron with a magnetic rigidity of 200 Tm (SIS-200). According to the preliminary design studies, this synchrotron would deliver a U^{+10} beam that will contain at least 10^{12} particles with a maximum energy of 1 GeV/u.

In this section we present hydrodynamic simulation re-

sults of implosion of multilayered cylindrical targets that contain a layer of frozen hydrogen and that are irradiated by the SIS-18 and SIS-200 beams, respectively. These calculations have been carried out using a two-dimensional hydrodynamic simulation code BIG-2 [4]. The numerics of this code is based on a Gudonov type scheme that has a second-order accuracy in space. It is an Eulerian code that uses a rectangular curvilinear adaptive moving grid. It can handle complex target geometry and it includes ion-energy deposition taking into account beam geometry. It also includes electron thermal conductivity and it allows for two different options for equation-of-state (EOS) data, namely, from the SESAME data Library and from a semiempirical data library [24].

In these calculations we use the SESAME equation-of-state (EOS) data for hydrogen while for lead we use the Chernogolovka semiempirical EOS data.

A. Super range multilayered target for the SIS-18 beam

The beam-target arrangement is shown in Fig. 1. The target consists of a solid hydrogen cylinder that is enclosed within a solid lead shell. In these calculations we assume that the target length $L = 3.0$ mm, the radius of the hydrogen region, $R_h = 0.5$ mm and the outer radius of the lead layer, $R_0 = 2.5$ mm. The right face of this target is irradiated by the ion beam that has a ring-shaped focal spot. The inner radius of the focus ring, R_{bi} is also $= 0.5$ mm while the outer ring radius, $R_{bo} = 1.5$ mm. Although the upgraded SIS-18 beam is expected to contain 2×10^{11} particles, our calculations show that one may carry out this experiment even with a lower number of particles. In these calculations we assume that the beam consists of 10^{11} ions of uranium with a particle energy of 200 MeV/u and the pulse duration is 50 ns. Moreover the power profile in time as well as the power deposition profile along the radial direction are parabolic.

Since previous simulations [1–3,7] showed that the SIS-18 beam will heat solid lead to about 10 eV, it is sufficient to consider the target as cold material and use cold range of ions in these calculations. The range of 200 MeV/u uranium ions in solid cold lead is about 1.7 mm [25]. The ions therefore penetrate about 1.7 mm into the lead from the right face towards the left. The Bragg peak thus lies at $L = 1.3$ mm. The energy is deposited in the lead region that creates a shell of very hot material around the frozen hydrogen cylinder. This hot lead shell has a length of 1.7 mm, an inner radius of 0.5 mm and an outer radius of 1.5 mm, as shown in Fig. 2(a) where we plot the specific energy deposition at $t = 50$ ns, a time when the beam has just delivered its total energy. It is seen that the Bragg peak lies at $L = 1.3$ mm and the maximum value of the specific energy deposition is 17 kJ/g that lies in the Bragg peak region at $r = 1.0$ mm. This corresponds to a specific power deposition of 0.34 Tw/g.

The energy deposited by the beam creates a high pressure region as shown in Fig. 2(b) which is also plotted at $t = 50$ ns. This pressure profile generates shock waves along the beam direction as well as along the target radius, inwards
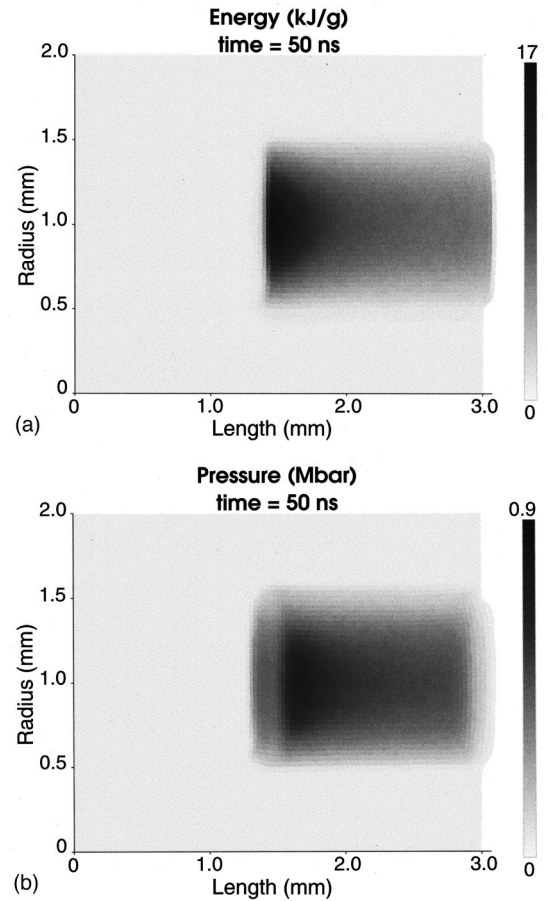
FIG. 2. (a) Specific energy deposition and (b) pressure in the target, created by 10^{11} particles of uranium 200 MeV/u, ring-shaped focal spot, inner radius$=0.5$ mm, outer radius$=1.5$ mm, pulse length$=50$ ns, at $t = 50$ ns.

and outwards. The radially inward propagating shock wave enters the hydrogen layer and compresses and heats the material as it converges towards the axis. Due to the cylindrical convergence effect, a higher temperature is generated along the axis. It is also important to note that the specific energy deposition is not uniform along the particle trajectory, being two times higher in the Bragg peak area compared to the rest of the absorption region. The strength and the speed of the shock front therefore varies accordingly and as a result of this the shock front arrives at the cylinder axis at different times and creates a nonuniform temperature profile along the axis. The shock propagation is followed by a strong adiabatic compression and the hydrogen-lead boundary slowly moves inwards as shown by Fig. 3 where we plot the target density at $t = 200$ ns.

It is interesting to note that this boundary moves faster in the region where the Bragg peak lies because in this region the energy deposition is much higher. This is indicated by the difference in the position of the lead-hydrogen boundary along axial direction below the deposition region ($L = 1.3$–3.0 mm). It is also seen that there is no compression of hydrogen between the Bragg peak region and the left face
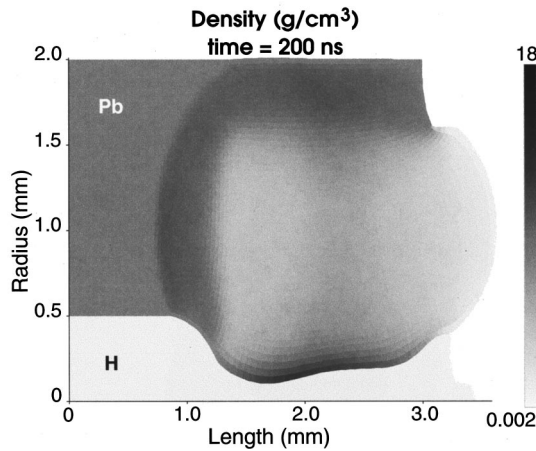
FIG. 3. Density on a length-radius plane at $t = 200$ ns.

of the cylinder which lies below the unheated part of the lead shell.

The compression of hydrogen enters the interesting phase of theoretically predicted physical conditions required for metallization at about $t = 240$ ns. In Figs. 4(a)–4(e) we plot the density, temperature, and pressure along cylinder length in the compressed hydrogen region at $r = 0.0$ mm (cylinder axis) at different times. Figure 4(a) shows that at $t = 240$ ns, between $L = 1.4$–1.7 mm, the pressure is above 2 Mbar, the density is about 0.8 g/cm^3 while the temperature is about 0.15 eV. Figure 4(b) shows that at $t = 245$ ns, between $L = 1.35$–1.6 mm, the pressure is between 2.0–4.5 Mbar the density is above 1 g/cm^3 while the temperature is about 0.3 eV. Figures 4(c) and 4(d) are plotted at $t = 250$ ns and 255 ns, respectively. These figures show similar physical conditions as Fig. 4(b), except that the maxima are shifted towards the left. Figure 4(e) which is plotted at $t = 260$ ns, shows the onset of the expansion phase. It is seen from these figures that the hydrogen remains in compressed state for about 20 ns, which is enough time to carry out the analysis.

In order to check the sensitivity of the results to variations in beam parameters we carried out calculations using different radii for the beam focal spot, while keeping the target dimensions fixed. In one case we assumed that $R_{bi} = 0.7$ mm and $R_{bo} = 1.7$ mm. In another calculation we allowed for an $R_{bi} = 0.8$ mm and an $R_{b0} = 1.8$ mm. The results are plotted in Figs. 5 and 6, respectively.

Figure 5 shows the density, temperature and pressure along the cylinder length in the compressed hydrogen region between $L = 1.4$ mm and 2.0 mm, at $r = 0.0$ mm (along cylinder axis), at $t = 330$ ns, corresponding to the former case. It is seen that between $L = 1.5$ mm and 1.8 mm, physical conditions necessary for the hydrogen metallization exist. These conditions last for about 20 ns.

Figure 6 shows the density, temperature, and pressure along the cylinder length in the compressed hydrogen region between $L = 1.4$ mm and 2.0 mm, at $r = 0.0$ mm (along cylinder axis), at $t = 370$ ns, for the latter case. It is seen that although we achieve physical conditions required for hydrogen metallization, the results are not so good as in the previous two cases.

The above study shows that the results obtained using this design are insensitive to significant variations in beam parameters. A similar study has also been done in which we keep the beam parameters fixed and alter the target parameters. We again found that the results are insensitive to significant variations in target parameters.

We note that as the radii of the beam focus are increased, the area of the focal spot increases and the specific energy as well as the specific power deposition decreases. If we keep the target radii fixed, the mass of lead that has to be imploded increases with R_{bi}. This slows the implosion as is seen from a comparison among Figs. 4, 5, and 6. If R_{bi} is made too large, the lead mass becomes too big to be driven effectively that makes the implosion inefficient.

We also note that the minimum thickness of the compressed hydrogen is about 30 micron. For diagnostic purposes, it may thus be more appropriate to study the optical properties of the sample rather than measuring the conductiity.

B. Subrange multilayered target for the SIS-200 beam

The considered SIS-200 design is expected to deliver a beam of uranium that will have at least 10^{12} particles. Although the maximum particle energy is expected to be 1 GeV/u, it is possible to operate the machine at a lower particle energy. We found that 400 MeV/u is a more suitable regime for our calculations. We also consider that the beam has a ring-type focal spot with an inner radius of 0.5 mm and an outer radius $= 2.0$ mm while the beam power deposition profile along the radial direction is parabolic. The pulse length is 50 ns and the power profile in time is also parabolic. The range of these ions in cold solid lead is about 4.3 mm [25].

In these calculations we consider the same beam-target geometry as shown in Fig. 1, namely, a multilayered cylinder that consists of a frozen layer of hydrogen which is enclosed in a thick lead shell. The length of this target, $L = 3.0$ mm, radius of hydrogen region, $R_h = 0.5$ mm and outer radius of the lead shell, $R_0 = 3.0$ mm.

Although the beam-target geometry as well as the target parameters in the two cases are the same, the targets work in a very different manner. This is because in the previous case of 200 MeV/u uranium ions, the ion range is 1.7 mm which is much shorter than the length of the target. The beam is completely stopped in the target and it is a ''super-range target.'' Due to the presence of the Bragg peak in the target, the energy deposition is highly nonuniform along the particle trajectory that leads to a nonuniform implosion of the hydrogen layer.

In the present case, on the other hand, the range of the 400 MeV/u uranium ions is larger than the target length. The ions therefore deposit part of their energy in the target and emerge from the left face with a reduced energy. This is a typical ''subrange target'' and the Bragg peak now lies outside the target. The energy deposition along the particle trajectory is nearly uniform that leads to an almost uniform compression of the entire hydrogen layer.

In Fig. 7 we plot the specific energy deposition along
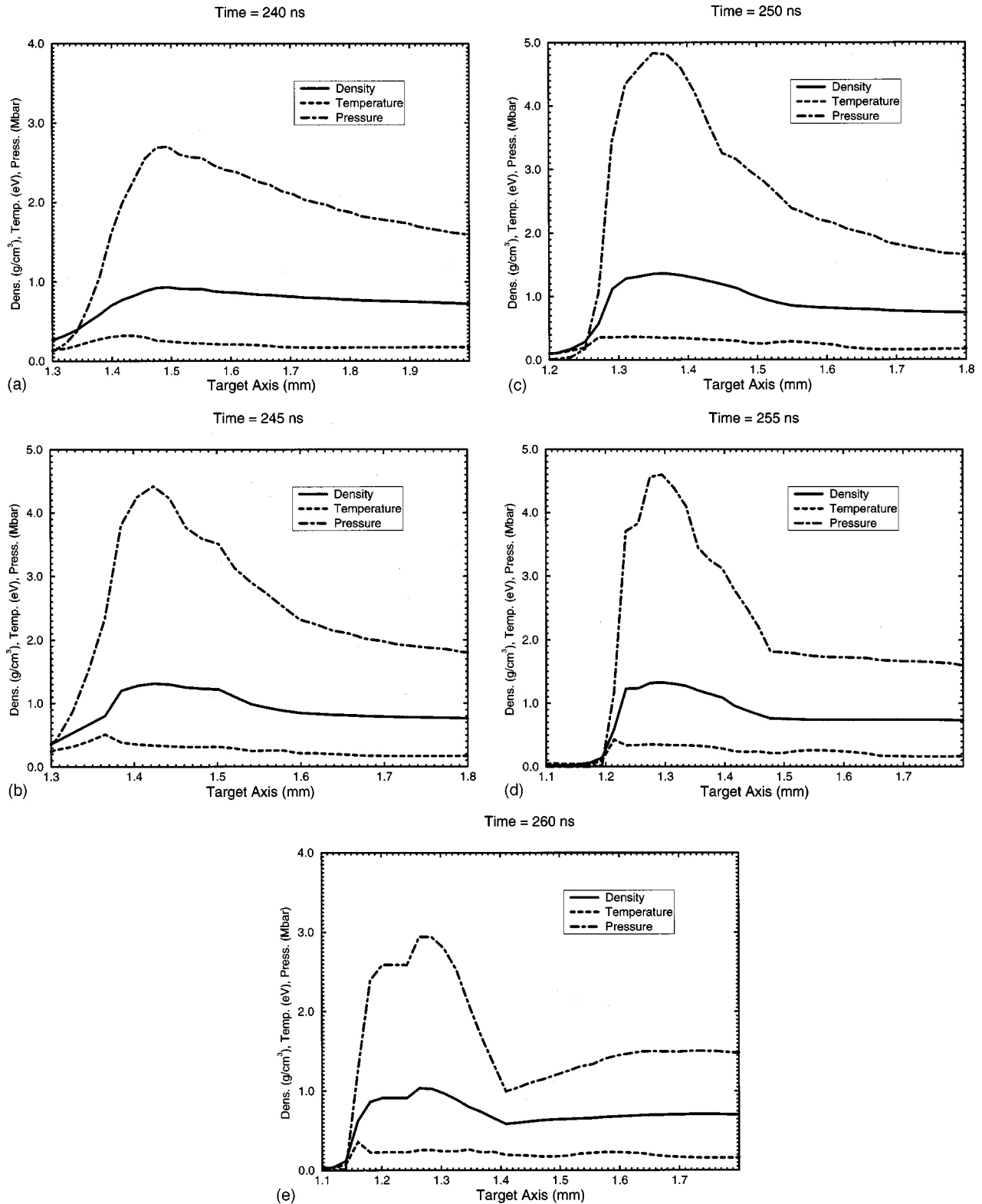
FIG. 4. Density, pressure, and temperature vs length at $r=0.0$ mm (axis) in compressed part of hydrogen, (a) at $t=240$ ns, (b) at $t=245$ ns, (c) at $t=250$ ns, (d) at $t=255$ ns, and (e) at $t=260$ ns.

length at $r=1.25$ mm (where maxima of the parabolic distribution lies), at $t=50$ ns (time when the beam has delivered its total energy). It is seen that the specific energy deposition is of the order of 30 kJ/g at $L=3.0$ that represents the beginning of the particle trajectory and is about 40 kJ/g at $L=0.0$ mm that lies at the end of the beam trajectory. One may therefore consider that the energy deposition along the target length is approximately uniform.

Time = 330 ns
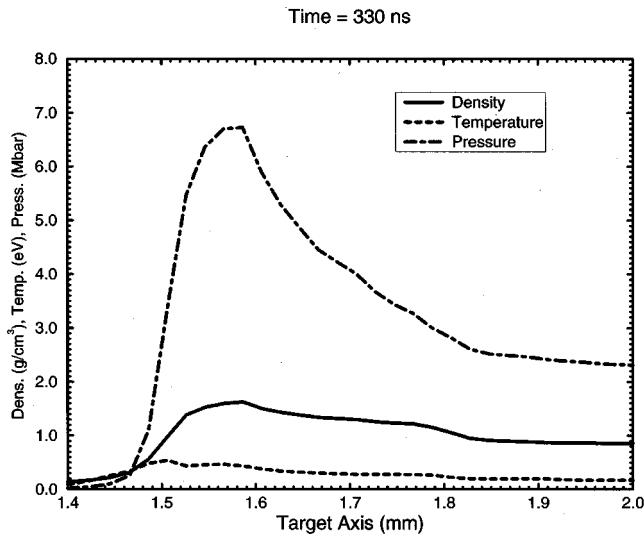
FIG. 5. Same as in Fig. 4, but at $t = 330$ ns, using an inner radius for focal spot$=0.7$ mm and an outer radius$=1.7$ mm.

The heated material from both faces of the lead cylinder expands in axial direction while shock waves are generated in radial direction, inwards as well as outwards. The inward moving shock wave heats and compresses the hydrogen as it converges towards the axis. The shock is reflected at the axis and a return shock is generated that propagates radially outward. The return shock is then reflected at the hydrogen-lead boundary which is slowly moving inward, thereby compressing the hydrogen layer. Due to the multiple shock reflection plus the slow adiabatic compression of the hydrogen layer, the density increases substantially, while the temperature remains low. In this beam-target configuration, the entire hydrogen layer is uniformly compressed, which is in contrast to the case presented in Sec. III A. This is shown in Fig. 8 where we plot the target density at $t = 100$ ns. It is seen that

Time = 370 ns
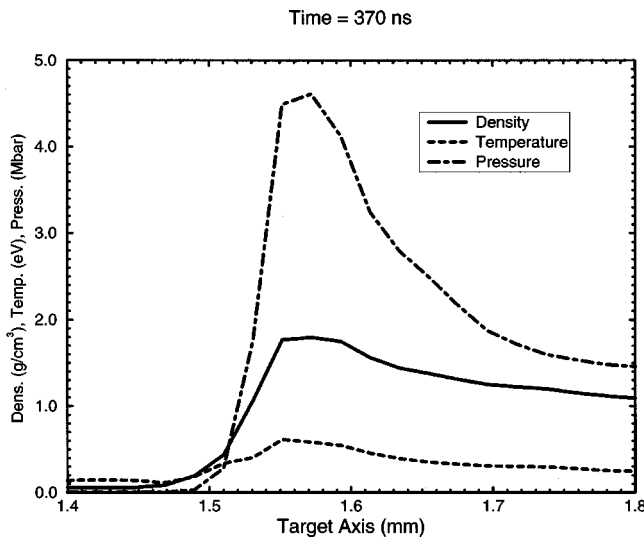
FIG. 6. Same as in Fig. 4, but at $t = 370$ ns, using an inner radius of focal spot$=0.8$ mm and an outer radius$=1.8$ mm.

Time = 50 ns, Pulse Length = 50 ns
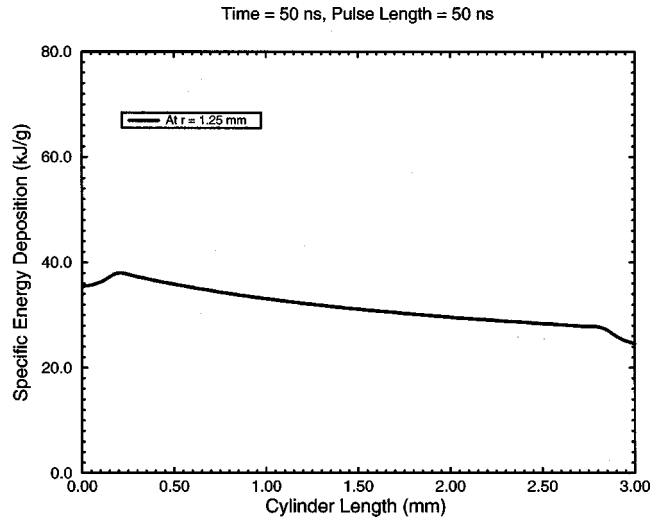
FIG. 7. Specific energy deposition along target length, at $r = 1.25$ mm at $t = 50$ ns, 10^{12} ions of uranium 400 MeV/u, annular focal spot, inner ring radius$=0.5$ mm, outer ring radius$=2.0$ mm and pulse length$=50$ ns.

by this time the hydrogen-lead boundary has moved from an initial position of 0.5 mm to 0.3 mm.

The compression of hydrogen enters the interesting regime of the predicted metallization conditions at 170 ns as shown by Fig. 9(a) where we plot the density, temperature, and pressure along the cylinder axis ($r = 0.0$ mm). It is seen that the density is about 0.9 g/cm^3, the pressure is about 2.5 Mbar and the temperature is of the order of 0.2 eV. Figure 9(b) shows the same variables as Fig. 9(a), but at $t = 180$ ns. It is seen that now the density is about 1.5 g/cm^3, the pressure is over 5 Mbar, while the temperature is about 0.4 eV.

Figure 9(c) again shows the same variables as Fig. 9(a), but at $t = 190$ ns. It is seen that conditions required for hydrogen metallization still exist in the target. In fact these
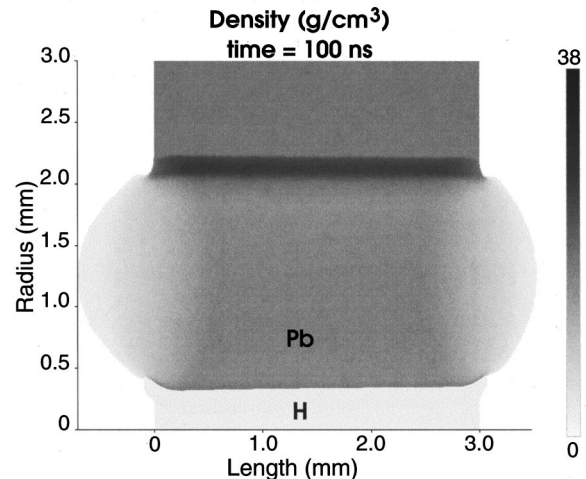
FIG. 8. Density on a length-radius plane at $t = 100$ ns.
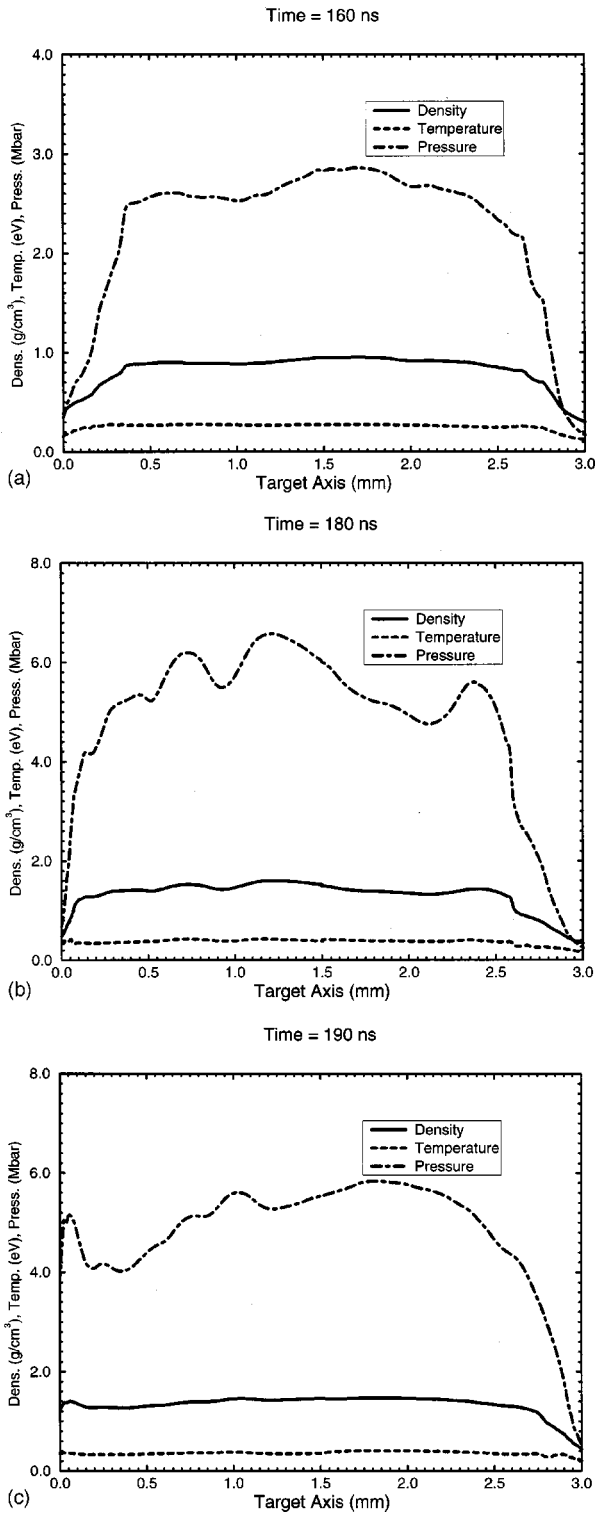
FIG. 9. Density, temperature, and pressure along the target axis (at $r = 0.0$ mm), (a) at $t = 160$ ns, (b) at $t = 180$ ns, and (c) at $t = 190$ ns.
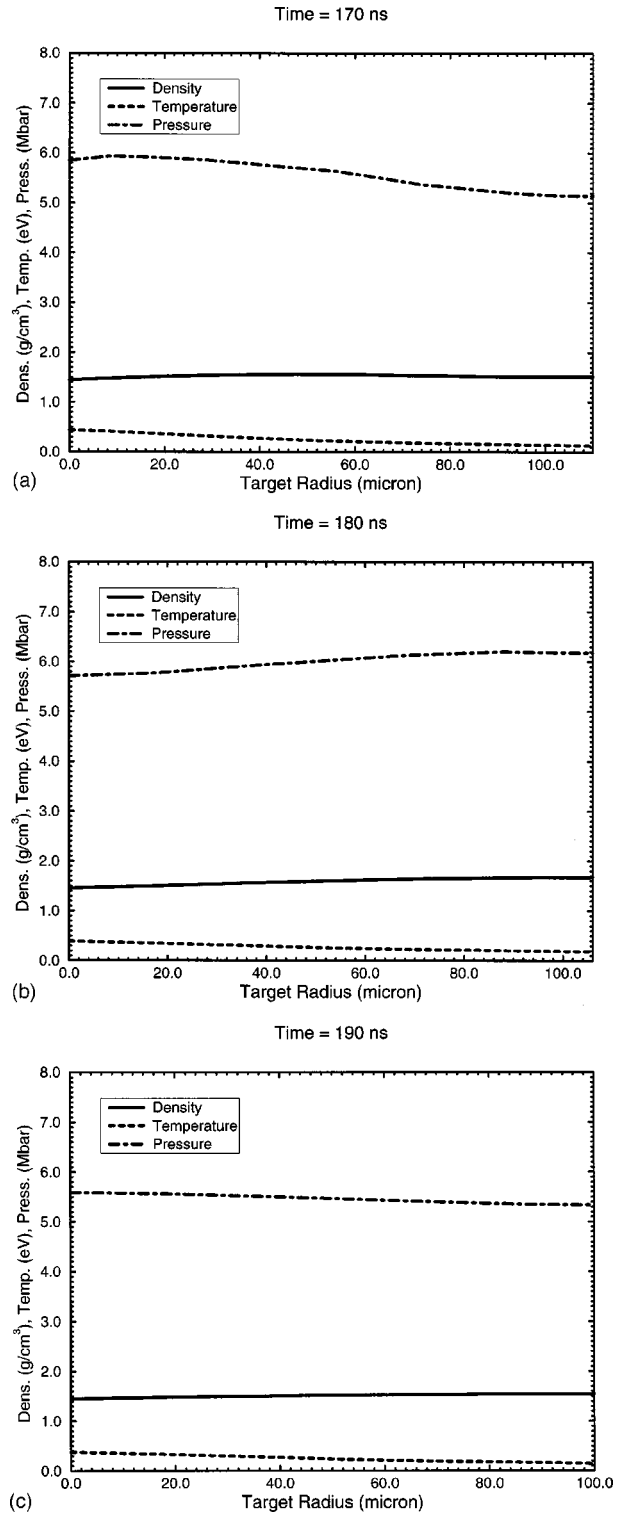
FIG. 10. Density, temperature, and pressure vs target radius at $L = 1.0$ mm, (a) at $t = 170$ ns, (b) at $t = 180$ ns, and (c) at $t = 190$ ns.

conditions last for up to 200 ns which means that one has about 40 ns to study the sample experimentally.

In Figs. 10(a)–10(c) we plot the density, temperature, and pressure along radius at $L = 1.0$ mm in the hydrogen region at $t = 170$ ns, 180 ns, and 190 ns, respectively. It is seen that at $t = 170$ ns, the radius of the compressed hydrogen cylinder is 110 microns and the compression is quite uniform. In the latter two figures, the radius has been reduced to 106 micron and 100 microns, respectively. This shows that the dimensions of this compressed hydrogen sample are reason-

ably large, which makes it relatively easy to diagnose the material.

We note that hydrogen is difficult to contain and when statically heated above 500 K, it diffuses into the walls of the containing vessel very rapidly. It is therefore very important that hydrogen sample is heated for a very short period of time. In our calculations, the time scale of the proposed experiment is of the order of a few hundred ns. This time scale is short enough to avoid loss of hydrogen through diffusion.

IV. SUMMARY AND CONCLUSIONS

We have shown with the help of two-dimensional hydrodynamic simulations that intense beams of energetic heavy ions may be used to create metallic hydrogen by imploding multilayered cylindrical targets that contain a layer of frozen hydrogen. In these calculations, we have considered a multilayered cylindrical target that is 3.0 mm long and that consists of a frozen hydrogen cylinder which is enclosed in a thick shell of solid lead. The radius of the hydrogen layer is 0.5 mm while the outer radius of the lead shell is 2.5 mm. The right face of this cylinder is irradiated by an ion beam which has an annular or ring-shaped focal spot that has an inner radius of 0.5 mm and an outer radius of 1.5 mm. The beam energy is deposited in the lead and a layer of hot, high pressure lead region is created around the hydrogen region. The high pressure in the lead layer launches a shock wave into the hydrogen that compresses the hydrogen as it converges on the axis. The shock is reflected at the axis and a return shock is generated that travels outward along the radial direction. The return shock is again reflected at the hydrogen-lead interface while this interface continues to move inward. As a result of this multiple shock reflection and slow adiabatic compression, the hydrogen density increases substantially, while the temperature remains low.

In this paper we report results using beams with two different parameters. In one case we consider a U^{+28} beam with 10^{11} particles having a particle energy of 200 MeV/u. Such a beam will be generated at the GSI Darmstadt heavy-ion synchrotron facilty, SIS-18, by end of the year 2001. The range of 200 MeV/u uranium ions is about 1.7 mm which is much smaller than the target length. This configuration therefore leads to implosion of a ''super-range target'' in which the entire beam is stopped. Our calculations show that it may be possible to achieve the theoretically predicted physical conditions required for hydrogen metallization. We achieve a density of about 1.5 g/cm^3, a pressure of about 4 Mbar and a temperature of the order of 0.4 eV. A systematic parameter study has also been carried out that has shown that the results are insensitive to significant changes in beam as well as target parameters.

GSI is also considering as a possible scenario for development of the accelerator facilities to build a synchrotron with a much higher magnetic rigidity of 200 Tm. Such a machine, SIS-200 will deliver a beam of U^{+10} that will contain at least 10^{12} particles with a particle energy of 1 GeV/u. It is also possible to operate this machine at a lower particle energy and we find that 400 MeV/u is more suitable for our calculations. Using this beam we simulated the hydrodynamic response of the same target as in the first case. The range of 400 MeV/u uranium ions in cold solid lead is about 4.3 mm. Therefore the ions deposit part of their energy in the target and emerge from the opposite face of the cylinder with a much reduced energy. This configuration therefore leads to implosion of a ''subrange target.'' Since the Bragg peak lies outside the target, the energy deposition along the particle trajectory is approximately uniform. This in turn leads to a nearly uniform compression of the hydrogen layer. The implosion leads to a density of about 1.5 g/cm^3 and a pressure of the order of 5 Mbar. The average temperature is low and is about 0.3 eV.

The second configuration is more attractive from the experimental point of view because the hydrogen is uniformly compressed and the sample dimensions are sufficiently large.

ACKNOWLEDGMENTS

[1] N. A. Tahir, D. H. H. Hoffmann, J. A. Maruhn, P. Spiller, and R. Bock, Phys. Rev. E **60**, 4715 (1999).

[2] N. A. Tahir, D. H. H. Hoffmann, A. Kozyreva, A. Shutov, J. A. Maruhn, U. Neuner, A. Tauschwitz, P. Spiller, and R. Bock, Phys. Rev. E **61**, 1975 (2000).

[3] N. A. Tahir, D. H. H. Hoffmann, A. Kozyreva, A. Shutov, J. A. Maruhn, U. Neuner, A. Tauschwitz, P. Spiller, and R. Bock, Phys. Rev. E **62**, 1224 (2000).

[4] V. E. Fortov, B. Goel, C.-D. Munz, A. L. Ni, A. V. Shutov, and O. Yu. Vorobiev, Nucl. Sci. Eng. **123**, 169 (1996).

[5] U. Ratzinger (unpublished).

[6] K. Blasche, O. Boine-Frankheim, H. Eickoff, M. Emmerling, B. Franczak, I. Hofmann, K. Kaspar, U. Ratzinder, and P. Spiller, Proceedings of the 6th European Part. Acc. Conf., EPAC-98, Stockholm (1998), p. 1347.

[7] N. A. Tahir, D. H. H. Hoffmann, J. A. Maruhn, K.-J. Lutz, and R. Bock, Phys. Plasmas **5**, 4426 (1998).

[8] E. Wigner and H. B. Huntigton, J. Chem. Phys. **3**, 764 (1935).

[9] C. Friedli and N. W. Ashcroft, Phys. Rev. B **16**, 662 (1977).

[10] T. W. Barbee, A. Garcia, M. L. Cohen, and J. L. Martins, Phys. Rev. Lett. **62**, 1150 (1989).

[11] N. W. Ashcroft, Phys. Rev. Lett. **21**, 1748 (1968).

[12] E. G. Brovman, Y. Kaygon, and A. Kholas, Sov. Phys. JETP **34**, 1300 (1972) [Zh. Eksp. Teor. Fiz. **61**, 2429 (1971)].

[13] H. K. Mao and R. J. Hemley, Science **244**, 1462 (1989).

[14] H. K. Mao and R. J. Hemley, Rev. Mod. Phys. **66**, 671 (1994).

[15] W. J. Nellis, A. C. Mitchell, P. C. McCandless, D. J. Erskine, and S. T. Weir, Phys. Rev. Lett. **68**, 2937 (1992).

[16] S. T. Weir, A. C. Mitchell, and W. J. Nellis, Phys. Rev. Lett. **76**, 1860 (1996).

[17] D. H. H. Hoffmann, K. Weyrich, H. Wahl, D. Gardes, R. Bimbot, and C. Fleurier, Phys. Rev. A **42**, 2313 (1990).

[18] J. Jacoby *et al.*, Phys. Rev. Lett. **65**, 2007 (1990).

[19] E. Boggasch, J. Jacoby, H. Wahl, K.-G. Dietrich, D. H. H. Hoffmann, W. Laux, M. Elfers, C. R. Haas, V. P. Dubenkov, and A. A. Golubev, Phys. Rev. Lett. **66**, 1705 (1991).

[20] K. G. Dietrich, D. H. H. Hoffmann, E. Boggash, J. Jacoby, H. Wahl, M. Elfers, C. R. Hass, and V. P. Dubenkov, Phys. Rev. Lett. **69**, 3623 (1992).

[21] S. Stöwe, R. Bock, M. Dornik, P. Spiller, M. Stetter, V. E. Fortov, V. Mintsev, M. Kulish, A. Shutov, V. Yakushev, B. Sharkov, A. Golubev, B. Bruynetkin, U. Funk, M. Geissel, D. H. H. Hoffmann, and N. A. Tahir, Nucl. Instrum. Methods Phys. Res. A **415**, 384 (1998).

[22] U. Funk, R. Bock, M. Dornik, M. Geissel, M. Stetter, S. Stöwe, N. A. Tahir, and D. H. H. Hoffmann, Nucl. Instrum. Methods Phys. Res. A **415**, 68 (1998).

[23] C. Stöckel, O. Boine-Frankheim, M. Geissel, M. Roth, H. Wetzler, W. Seelig, O. Iwase, P. Spiller, R. Bock, W. Süß, and D. H. H. Hoffmann, Nucl. Instrum. Methods Phys. Res. A **415**, 558 (1998).

[24] I. V. Lomonosov, A. V. Bushman and V. E. Fortov, in *High-Pressure Science and Technology* (AIP Press, New York, 1994), Part 1, p. 117, edited by S. C. Schmidt, J. W. Schaner, G. A. Samara and M. Ross.

[25] J. F. Ziegler, J. P. Biersack, and U. Littmark, *The Stopping and Ranges of Ions in Solids* (Pergamon Press, New York, 1996).